Long-range triggered earthquakes that continue after the wave train passes

Emily E. Brodsky[1]

Received 17 April 2006; revised 5 June 2006; accepted 27 June 2006; published 10 August 2006.

[1] Large earthquakes can trigger distant earthquakes in geothermal areas. Some triggered earthquakes happen while the surface waves pass through a site, but others occur hours or even days later. Does this prolonged seismicity require a special mechanism to store the stress from the seismic waves that differs from ordinary aftershock mechanisms? These questions have driven studies of long-range triggering since the phenomenon's discovery. Here I attempt to answer the questions by examining the statistics of triggered sequences. Two separate observations are consistent with the prolonged sequences being simply local aftershocks of earthquakes triggered early in the wave train. First, the sequences obey Omori's Law over both short (1 hour) and longer (5 day) time intervals. Secondly, the number of observed triggered earthquakes in the first hour after the wave train can be predicted from the number of earthquakes triggered during the wave train. Even the very vigorous 10-day triggering at Long Valley from the 1992 Landers M_w 7.3 earthquakes can be interpreted as the aftershocks of either a local $M \approx 4.1$ earthquake or an equivalent combination of several smaller mainshocks. Therefore, long-range triggering does not need to include a mechanism to produce sustained stresses other than the process that generates aftershocks of the earthquakes that occur while the wave train is passing. **Citation:** Brodsky, E. E. (2006), Long-range triggered earthquakes that continue after the wave train passes, *Geophys. Res. Lett.*, *33*, L15313, doi:10.1029/2006GL026605.

1. Introduction

[2] Seismic waves trigger earthquakes. For instance, as surface waves passed through geothermal sites like Yellowstone and Long Valley after earthquakes like the 1992 M_w 7.3 Landers and 2002 M_w 7.9 Denali events, local earthquakes flared up [*Hill et al.*, 1993; *Stark and Davis*, 1996; *Prejean et al.*, 2004]. However, the increased seismicity did not end with the end of the surface waves. It continued for an hour in some places and in other places for over a week. How do the transient waves of the far-field earthquakes make such a sustained response? This sustained response has been taken as a key piece of evidence for or against various triggering mechanisms [*Gomberg*, 2001; *Brodsky et al.*, 1998]. Others have suggested that a handful of earthquakes are triggered locally during the passage of the seismic waves and all subsequent earthquakes are aftershocks of these first, locally triggered events [*Hough and Kanamori*, 2002]. Figure 1 illustrates the problem. Are the late triggered earthquakes aftershocks of the waveform triggered ones?

[3] Here I show that in the best-documented cases, the sustained seismicity from long-range triggering (>100 km from the mainshock) in geothermal areas has the same behavior as ordinary aftershock sequences. The data will show that: (1) Long-range triggered sequences follow Omori's law and (2) The number of events triggered over 1 hour after the mainshock is consistent with number of aftershocks expected from earthquakes triggered during the passage of the seismic waves. Taken together, the data is fully consistent with the sustained long-range triggering occurring by the same process that sustains aftershock sequences in general. No more complicated process is required by this data set.

2. Omori's Law

[4] Local earthquakes are poorly cataloged after a large earthquake, so I use broadband waveforms from individual stations to count the number of earthquakes near the station immediately after a main shock (Figure 2).

[5] Figure 2 shows all documented long-range triggering sequences with more than 35 local events recorded on a broadband seismometers closer than 30 km away during the first hour after the arrival of the surface waves. There are only a handful of these cases. Two records come from a recent deployment of two Guralp 6TD seismometers (30 s corner frequency) in The Geysers geothermal field in Northern California during the 6/25/2005 Mendocino M_w7.2 earthquake and the third is from a permanent station.

[6] A straight line on Figure 2 indicates an Omori's law with p-value of 1; that is, the cumulative number of earthquakes is

$$N = \int_{T_0}^{T} \frac{K}{t} dt = K' \log T + C \qquad (1)$$

where T is the time after the earthquake origin time T_0 and K, K' and C are constants.

[7] Each individual sequence in Figure 2 follows an Omori's law decay of the form of equation (1). The fits are quite good as demonstrated by the correlation coefficient r which exceeds 97% for all cases. The fit reduces the sum of the residuals by a factor of 2.4 for the Geysers relative to a linear-time fit (constant seismicity rate) and a factor of 1.8 for Long Valley. Oddly, the fit is very good even during the first ~400 s of the Denali-Long Valley sequence while the seismic wave excitation is still continuing.

[8] Longer duration triggered sequences are in Figure 3. The identification of these sequences as triggered earth-

[1]Department of Earth Sciences, University of California, Santa Cruz, California, USA.

0094-8276/06/2006GL026605

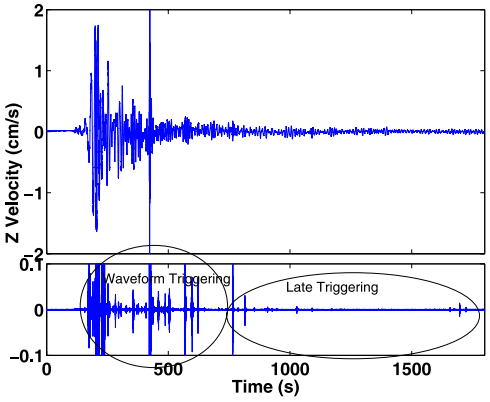

Figure 1. Vertical seismogram from the 2005 Mendocino earthquake recorded with a temporary deployment of broadband seismometers in The Geysers: (top) raw recording and (bottom) high-pass filtered at 7 Hz to show locally triggered earthquakes. The focus of this paper is whether or not the earthquakes labeled "late triggering" are aftershocks of those labeled "waveform triggering."

quakes is discussed elsewhere [*Hill et al.*, 1993; *Prejean et al.*, 2004]. All sequences with ≥100 cataloged earthquakes within 40 km and 5 days are included. The instantaneous rate is estimated using the nearest neighbor method which produces one rate measurement for each earthquake [*Silverman*, 1986]. Data is fit with a modified Omori's Law of

$$dN/dt = K/t^p \tag{2}$$

for times from the origin time of the earthquakes to when the seismicity rate reaches 50% of the average background rate. Once the aftershock rate approaches the background rate, other, non-related sequences are expected to overcome

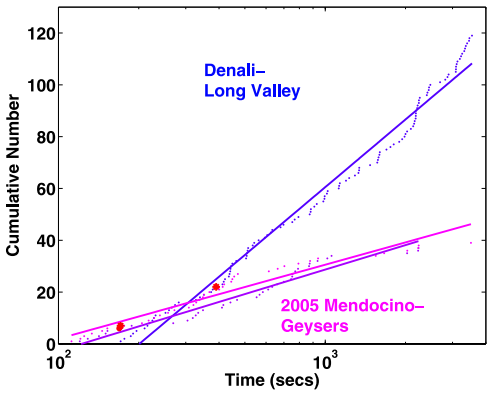

Figure 2. Cumulative number of earthquakes as counted from waveforms for broadband deployments near (<30 km) robust (>35 earthquakes) triggered sequences in the first hour after the arrival of the surface waves. Time 0 is the time of the arrival of the surface waves. Stars indicate the end of the mainshock wave trains. Geysers seismic data is from temporary deployments of two Guralp CMG-6TD seismometers and Long Valley data is from Univ. of Nevada broadband seismic station OMM.

the Omori's Law effect. For the Landers-Geysers and Denali-Yellowstone sequences, the best-fit values of p are 1.03 ± 0.03 and 0.98 ± 0.07, respectively, with significance >99%. This result is consistent with the earlier work of *Husen et al.* [2004] who fit the same Yellowstone data from the time of the Denali earthquake through 30 days with p = 1.02 ± 0.07 using a different statistical method.

[9] The Landers-Long Valley sequence is more complex. Prior to ~0.4 days, the data appears to be incomplete at low magnitudes (Figure 4) possibly due to the ongoing Landers aftershock sequence. If there is a variable completeness threshold in time, then early and late data should separately follow Omori's Law with the same value of p but different values of K. This is the case. Separately fitting the data for $t < 0.2$ days and $t > 0.4$ days, yields values of p of 0.95 ± 0.17 and 0.96 ± 0.12 for each set, respectively. If the whole time period is taken together for $M > 2$, the sparse data is best fit with p = 1.16 ± 0.17.

[10] In summary, both the short and long-term data are consistent with Omori's Law (Figures 2 and 3). In some cases, the Omori's Law trend begins while the shaking was still occurring. This rate decay suggests that each entire prolonged sequence may be simply an aftershock sequence of mainshocks that occurred locally during the shaking.

3. Productivity

[11] If the late-triggered earthquakes are aftershocks of the waveform-triggered ones, then the number of late-

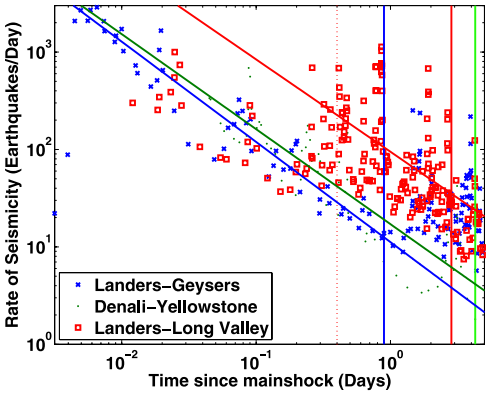

Figure 3. Seismicity rate of sequences with >100 cataloged earthquakes within 5 days. Solid lines show Omori's Law with best-fit values (equation (2)). (For Landers-Long Valley, the best-fit is on the >0.4 day data.) Vertical lines show times at which the seismicity rate reaches 50% of background rate for the sequence of the corresponding color. Background rates are simple averages of seismicity at each site in the years bracketing the triggering earthquake. The dotted line separates the Landers-Long Valley data into times of differing completeness as discussed in the text. Earthquake catalog data is from the Advanced National Seismic System (ANSS) catalog for Long Valley and Yellowstone and from the local Unocal catalog for The Geysers. Seismicity rate is smoothed with a 2-point running average. Only earthquakes above the completeness threshold are included. Cusps in the seismicity rate are secondary aftershock sequences.

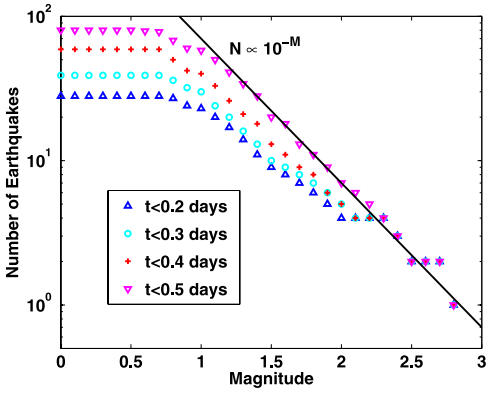

Figure 4. Cumulative magnitude-frequency distribution for Long Valley earthquakes for time intervals following the Landers earthquake. The data does not follow a typical Gutenberg-Richter distribution until 0.5 days after Landers which suggests that the early time data may be incomplete for $1 < M < 2$.

triggered earthquakes should be a function of the magnitude of the waveform-triggered earthquakes. Given information about the usual productivity of aftershocks in a region and the magnitude of the earthquakes during the waveform, one should be able to predict the number of late-triggered earthquakes. Making this prediction requires a model for aftershock productivity as a function of mainshock magnitude as well as a site with excellent coverage for both calibrating the model and observing the wavetrain triggered sequences. Here I use a standard model of aftershock productivity calibrated with 11 years of data from The Geysers to perform this exercise.

[12] On average, the number of aftershocks N observed on the local network produced by a local mainshock magnitude M is

$$N = C10^{\alpha M} \tag{3}$$

where C and α are constants [*Felzer et al.*, 2004; *Helmstetter et al.*, 2005]. Figure 5 shows the typical productivity of small mainshocks at the Geysers based on local short-period data over an 11 year period excluding the times of the regional earthquakes to be studied. The figure records the mean number of earthquakes above the completeness threshold (local Unocal magnitude 0.5) within 15 km and an hour following mainshocks of magnitude M. Mainshocks are defined as earthquakes that have no larger earthquake within 1 day prior. This primitive mainshock separation criterion may not recover the true, physical productivity of each aftershock sequence, but it does provide an empirical method to measure the apparent productivity of the catalog. The observable apparent productivity is adequate for the prediction of late-triggered earthquakes from the waveform-triggered mainshocks because: (1) Contamination from unrelated sequences is just as likely to occur at the arbitrary time of the remote triggering as during any other time in the catalog and (2) The values of productivity are only used in the magnitude calibration range, so trade-offs between α and C are unimportant in this application. The 3495 disjoint sequences used in Figure 5 follow equation (3). The best-fit values of α is 0.6 ± 0.02 and C is 0.2 ± 0.02 where the errors are the standard deviation of 1500 bootstrap trials.

[13] Using the magnitudes of the earthquakes in a hand-picked catalog for the 10 minutes following 9 regional earthquakes and the calibration in Figure 5, I predict the number of earthquakes in the next hour (Figure 6). Ten minutes covers the extended coda for the large regional events as can be seen in Figure 1. Each earthquake during the wavetrain is treated as a separate mainshock. The total predicted number of aftershocks is the sum of the contributions from each wavetrain triggered earthquake.

[14] The observed number of events fits the predictions with 98% significance. Several cases have 10–20% under-predictions of the sustained seismicity which might be attributable to catalog incompleteness during the waveforms. The

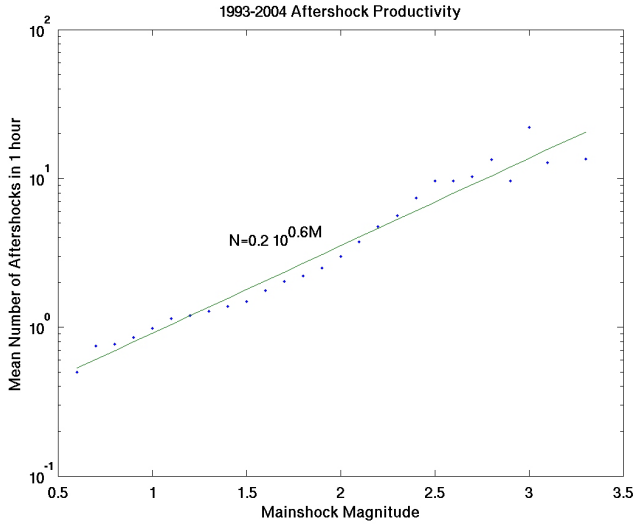

Figure 5. Number of earthquakes at The Geysers within one hour of mainshocks of magnitude M. Magnitudes are local Unocal network magnitudes which are typically depressed ~0.5 units from ANSS.

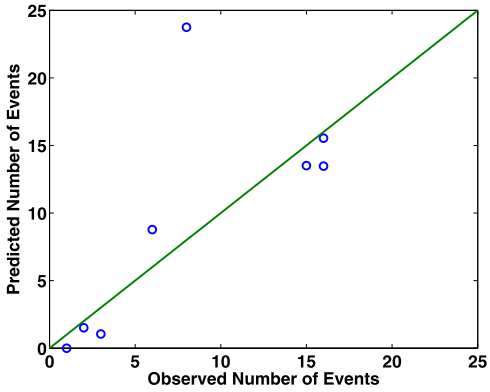

Figure 6. Predicted and observed number of earthquakes at The Geysers within 1 hour after distance mainshocks. Studied earthquakes were: 1992 M_w7.3 Landers, 1993 M_w6.0 Klamath Falls, 1994 M_w7.0 Mendocino, 1994 M_w6.6 Northridge, 1999 M_w7.1 Hector Mine, 2002 M_w7.8 Denali, 2003 M_w6.6 San Simeon, 2003 M_w8.3 Tokachi-Oki, 2005 M_w7.2 Mendocino. The number of predicted and observed earthquakes for Northridge and Klamath Falls are identical, so the points lie on top of each other in this figure.

outlier is the 1994 Mendocino earthquake which had fewer than expected earthquakes after the waves passed. At least 80% of the triggered earthquakes can be explained without any sustained process other than local aftershock generation.

4. Long Valley and Landers: A Counter-Example?

[15] The most prolonged example of long-range triggering is Landers at Long Valley, which lasted 10 days. At first glance, this sequence may appear to be a counter-example to the hypothesis that prolonged triggering is a local aftershock sequence. Here I show that the statistics of the sequence do not contradict the hypothesis and the prolonged triggering is consistent with a locally triggered aftershock sequence.

[16] As shown above, the sequence follows Omori's Law. No local seismometers remained operational and on-scale during the Landers waves, so the productivity prediction performed in Figure 6 is impossible for this data set. Instead, I perform the inverse exercise of predicting the magnitude of the largest local earthquakes during the wave train from the total number of earthquakes. For Long Valley from 1988–1999, I find $\alpha = 0.5 \pm 0.05$ and $C = 1.8 \pm 0.6$ for $M \geq 1$ earthquakes between 0.2 and 10 days after the mainshock (Main shocks are again defined as earthquakes with no larger earthquake 1 day prior; Errors are again 1 standard deviation on 1500 bootstraps).

[17] The observed number of earthquakes (208) is consistent with the entire sequence being triggering by an ~M4.1 local earthquake. Alternatively, several smaller earthquakes during the wave train could have an equivalent effect. For instance, three M_L3.1 earthquakes would suffice. Propagating the errors on α and C yields a range for the equivalent mainshock magnitude of M = 3.5–5.0.

[18] Magnitude 3–4 earthquakes in Long Valley could be hidden in the wave train of the Landers earthquake. The closest functioning broadband seismometer was ~140 km away. The short-period seismometers were too saturated during the main part of the Rayleigh wave to show local events even with very aggressive filtering. Shaking during the Landers earthquake woke people in the Long Valley area and would not necessarily be discernible from shaking originating locally.

[19] The observed deformation at Long Valley is also consistent with a local earthquake [*Johnston et al.*, 1995]. *Roeloffs et al.* [2003] observed that the strainmeter record of deformation at Long Valley from Landers was nearly identical to deformation from a local M4.9 earthquake.

[20] Other potential counter-examples are late large events that produce bursts of seismicity several days after the mainshock. Examples include the Denali-triggered earthquakes at Long Valley, Rainier and Yellowstone and the M_L5.6 Little Skull Mountain earthquake a day after the Landers earthquake [*Prejean et al.*, 2004; *Smith et al.*, 2001]. All of these sites had small earthquakes that began as soon as the seismic waves from the mainshock passed. Like all aftershock sequences, the continuing seismicity should have bursts of activity from large secondary aftershocks (See, for example, the cusps in Figure 3). The late bursts may be particularly large secondary aftershocks of the sequences that began with the passage of the surface waves.

5. Spatial Distribution

[21] Locations are too poor to definitively constrain the location of late triggered earthquakes relative to early ones. At The Geysers, the earthquake location errors during the wave train are much higher than the usual 0.7 km average horizontal error.

6. Conclusion

[22] For the analyzed sequences, the late triggered events appear to be aftershocks of the earthquakes triggered during the passage of the seismic waves. No sustained stress beyond the usual aftershock process is required. More complicated processes might occur, but there is nothing in the data that requires them.

[23] Transient triggering by the dynamic stresses of the Rayleigh waves followed by local static stress triggering of aftershocks would be consistent with the data presented here. However, other studies [*Felzer and Brodsky*, 2006] indicate that aftershocks may also be triggered by seismic waves. In that case, a sustained stress mechanism is still necessary for the aftershock process. Geothermal areas may be more susceptible to triggering from shaking than ordinary crust [*Brodsky et al.*, 2003; *Manga and Brodsky*, 2006], but once started, the triggered sequence proceeds like any other series of aftershocks. The conclusion of this study is that the prolonged nature of long-range triggered sequences is no more (or less) mysterious than the prolonged nature of aftershock sequences in general.

[24] **Acknowledgments.** Many thanks to R. Haught, W. Mooney, R. Sell and M. Stark for making the field deployments happen. M. Walters picked the Geysers short-period records. Additional catalog and waveform data is from ANSS, NCEDC and IRIS. The work was supported in part by NSF. Constructive reviews from J. Gomberg and D. Marsan improved the paper.

References

Brodsky, E. E., B. Sturtevant, and H. Kanamori (1998), Earthquake, volcanoes and rectified diffusion, *J. Geophys. Res.*, *103*, 23,827–23,838.

Brodsky, E. E., E. Roeloffs, D. Woodcock, I. Gall, and M. Manga (2003), A mechanism for sustained groundwater pressure changes induced by distant earthquakes, *J. Geophys. Res.*, *108*(B8), 2390, doi:10.1029/2002JB002321.

Felzer, K. R., and E. E. Brodsky (2006), Evidence for dynamic aftershock triggering from earthquake densities, *Nature*, *441*, 735–738.

Felzer, K., R. Abercrombie, and G. Ekstrom (2004), A common origin for aftershocks, foreshocks, and multiplets, *Bull. Seismol. Soc. Am.*, *94*, 88–98.

Gomberg, J. (2001), The failure of earthquake failure models, *J. Geophys. Res.*, *106*, 16,253–16,263.

Helmstetter, A., Y. Y. Kagan, and D. D. Jackson (2005), Importance of small earthquakes for stress transfers and earthquake triggering, *J. Geophys. Res.*, *110*, B05S08, doi:10.1029/2004JB003286.

Hill, D. P., et al. (1993), Seismicity remotely triggered by the magnitude 7.3 Landers, California, earthquake, *Science*, *260*, 1617–1623.

Hough, S., and H. Kanamori (2002), Source properties of earthquakes near the Salton Sea triggered by the 16 October 1999 M 7.1 Hector Mine, California, earthquake, *Bull. Seismol. Soc. Am.*, *92*, 1281–1289.

Husen, S., S. Wiemer, and R. Smith (2004), Remotely triggered seismicity in the Yellowstone National Park region by the 2002 Mw = 7.9 Denali Fault earthquake, Alaska, *Bull. Seismol. Soc. Am.*, *94*, S317–S331.

Johnston, M. J. S., D. P. Hill, A. T. Linde, J. Langbein, and R. Bilham (1995), Transient deformation during triggered seismicity from the 28 June 1992 M_w = 7.3 Landers earthquake at Long Valley volcanic caldera, California, *Bull. Seismol. Soc. Am.*, *85*, 787–795.

Manga, M., and E. E. Brodsky (2006), Seismic triggering of eruptions in the far field: Volcanoes and geysers, *Annu. Rev. Earth Planet. Sci.*, *34*, 263–291.

Prejean, S. G., et al. (2004), Observations of remotely triggered seismicity on the United States West Coast following the M7.9 Denali Fault earthquake, *Bull. Seismol. Soc. Am.*, *94*, S348–S359.

Roeloffs, E., M. Sneed, D. L. Galloway, M. Storey, C. D. Farrar, J. Howle, and J. Hughes (2003), Water-level changes induced by local and distant earthquakes at Long Valley caldera, California, *J. Volcanol. Geotherm. Res.*, *127*(3–4), 269–303.

Silverman, B. (1986), *Density Estimation for Statistics and Data Analysis*, CRC Press, Boca Raton, Fla.

Smith, K. D., J. N. Brune, D. dePolo, M. K. Savage, R. Anooshehpoor, and A. F. Sheehan (2001), The 1992 Little Skull Mountain earthquake sequence, southern Nevada Test Site, *Bull. Seismol. Soc. Am.*, *91*, 1595–1606.

Stark, M. A., and S. D. Davis (1996), Remotely triggered microearthquakes at The Geysers geothermal field, California, *Geophys. Res. Let.*, *23*, 945–948.

E. E. Brodsky, Department of Earth Sci., UC Santa Cruz, Santa Cruz, CA 95060, USA. (brodsky@es.ucsc.edu)